Superficies y Vacío ***19(3)****, 1-11, septiembre de 2006* *©Sociedad Mexicana de Ciencia y Tecnología de Superficies y Materiales*

Polarization-sensitive optical properties of metallic and semiconducting nanowires

Harry E. Ruda, Alexander Shik
Centre for Advanced Nanotechnology, University of Toronto
Toronto M5S 3E4, Canada
(Recibido: 10 de febrero de 2006; Aceptado: 25 de agosto de 2006)

Polarization phenomena in the optical absorption and emission of metallic, semiconducting or composite nanowires and nanorods are considered theoretically. Most nanowire-based structures are characterized by a dramatic difference in dielectric constant ε between their material and environment. Due to image forces caused by such ε mismatch, coefficients of optical absorption and emission become essentially different for light polarized parallel or perpendicular to the nanowire axis. As a result, the intensity and spectra of absorption, luminescence, luminescence excitation, and photoconductivity in single nanowires or arrays of parallel nanowires are strongly polarization-sensitive. In light-emitting nanowire core-shell structures, the re-distribution of a.c. electric field caused by the image forces may result in essential enhancing of core luminescence in frequency regions corresponding to luminescence from the semiconducting core or when the frequency of optical excitation coincides to the frequency of the plasmon resonance in the metallic shell. In random nanowire arrays, the effects described above may result in "polarization memory", where polarization of luminescence is determined by the polarization of the exciting light. Recent experimental data on "polarization memory" in CdSe/ZnS nanorods are presented.

Keywords: Manowires; Optical properties; Semiconductor

1. Introduction

The paper is devoted to optical phenomena in nanowires having a dielectric constant ε essentially different from that of their environment ε_0, when polarization effects (image forces) play an important role. This model describes semiconductor nanowires (with typical ε ~ 10) grown either in a free-standing fashion from catalyst particle nano-islands (see, e.g., [1]) or in a dielectric template with cylindrical pores [2], metallic nanowires where ε also differs noticeably from ε_0 and, besides, has a complex character and frequency dispersion, and composite core-shell nanostructures feasibility of which has been recently demonstrated experimentally [3,4].

In this paper, we consider the influence of image forces on the intensity of the optically-induced electric field inside nanowires, which, in turn, determines all light-induced phenomena, such as optical absorption, luminescence, and photoconductivity. We show that even in relatively thick nanowires, where size effects are not significant and energy spectrum, as well as transport coefficeints, are isotropic, the difference between ε and ε_0 results in a strong dependence of the above-mentioned phenomena on the polarization of the exciting light. Similarly, light emitted by such nanowires appears to be strongly polarized, even if the probability of the corresponding optical transitions is independent of the orientation of the effective dipole moment.

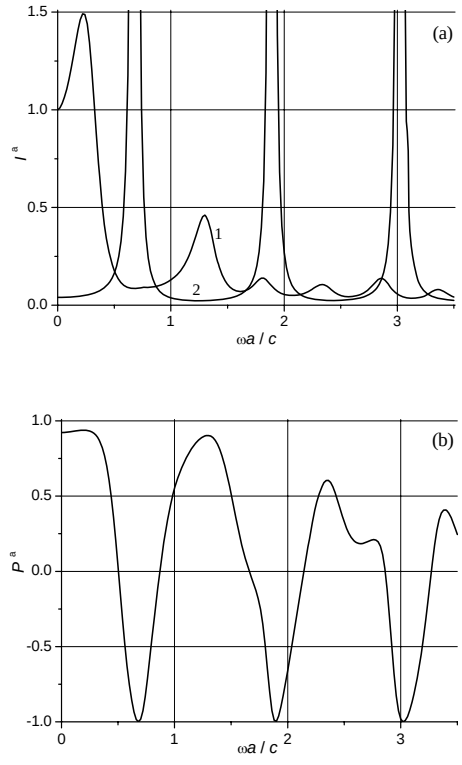

Figure 1. (a) – spectral dependence of the integral light intensity in a nanowire with ε = 9, ε_0 = 1 for the light polarized parallel to nanowires, $I_{\parallel}^{a}$ (1) and perpendicular to nanowires, $I_{\perp}^{a}$ (2), in units of $\pi a^2 E_0^2$; (b) – spectral dependence of the polarization ratio P^a in the same nanowire.

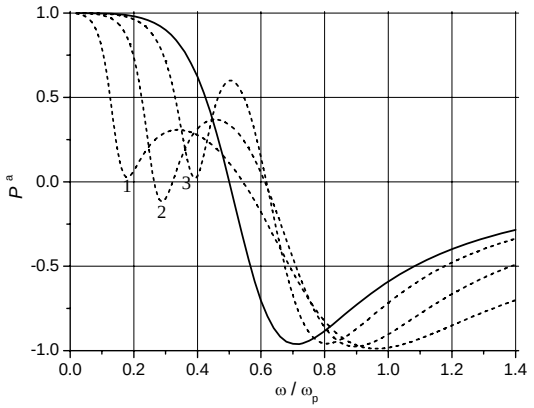

Figure 2. Absorption anisotropy P^a for a metallic nanowire (solid curve) and core-shell structures with p = 0.2 (1); 0.5 (2); 0.8 (3) at $\varepsilon_1 = 3$, $\nu = 0.1\omega_p$.

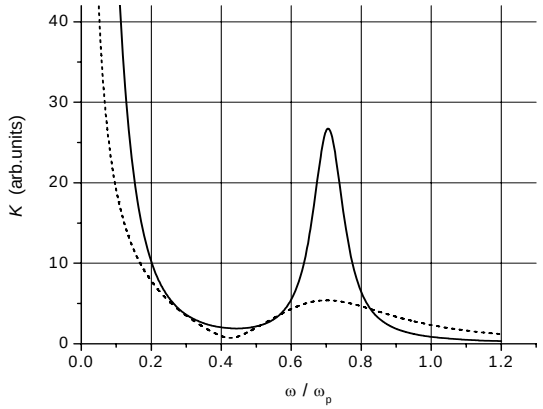

Figure 3. Absorption spectra of randomly oriented metallic nanowires at $\nu = 0.1\omega_p$ (solid curve) and $\nu = 0.5\omega_p$ (dashed curve).

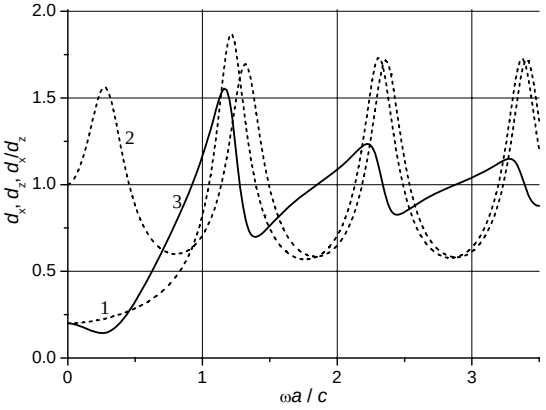

Figure 4. Spectral dependence of the effective dipoles d_x (1) and d_z (2) (in units of d_0) and of the ratio d_x/d_z (3) for a nanowire with $\varepsilon = 9$, $\varepsilon_0 = 1$.

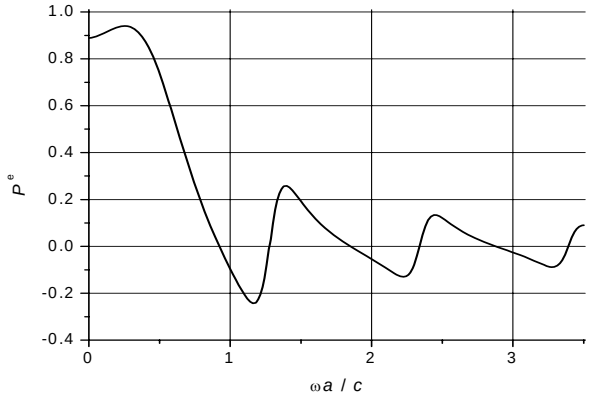

Figure 5. Spectral dependence of the polarization ratio P^a for luminescence from a nanowire with $\varepsilon = 9$, $\varepsilon_0 = 1$.

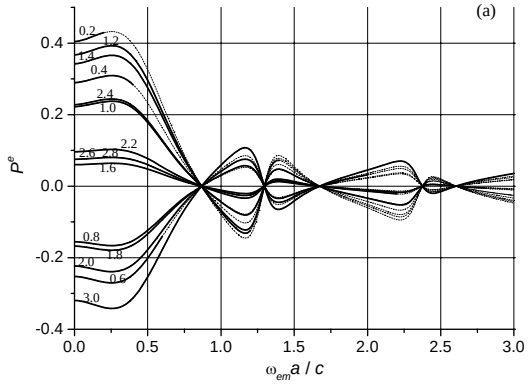

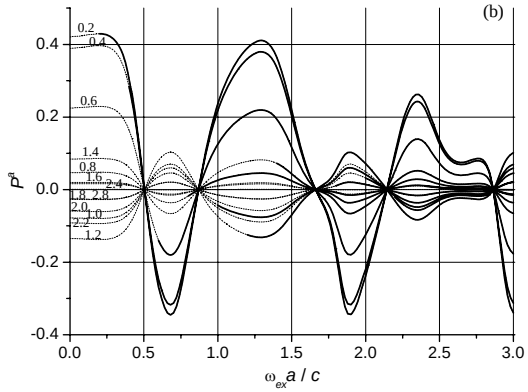

Figure 6. Polarization ratio of photoluminescence for a random system of nanowires with $\varepsilon = 9$, $\varepsilon_0 = 1$. (a) – luminescence spectra $P^e(\omega_{em})$ for different ω_{ex}. Figures at the curves indicate the values $\omega_{ex}a/c$. The curves corresponding to $\omega_{ex}a/c = 2.6$ and $\omega_{ex}a/c = 2.8$ practically coincide. (b) – excitation spectra $P^a(\omega_{ex})$ for different ω_{em}. Figures at the curves indicate the values of $\omega_{em}a/c$. The curves corresponding to $\omega_{em}a/c = 1.8$ and $\omega_{em}a/c = 2.8$ practically coincide. For $\omega_{em}a/c = 2.6$ polarization is very close to zero and not presented at the figure.

2. Polarization of absorption

2.1. Semiconductor nanowires

If a cylindrical wire is placed in external electric field $\mathbf{E_0}$, its parallel component, E_7, remains the same inside a wire while the component normal to the wire axis, $E_\perp$, will be essentially changed [5]:

$$E_{\parallel} = E_{0\parallel}; \qquad E_{\perp} = \frac{2\varepsilon_0}{\varepsilon + \varepsilon_0} E_{0\perp}. \tag{1}$$

For $\varepsilon > \varepsilon_0$, Eq.(1) means that the amplitude of the high-frequency electric field and, hence, the probability of optical transitions in a nanowire depend dramatically on the light polarization, acquiring maximal values for light with polarization parallel to the nanowire axis. The practical consequence of this effect is a strong dependence of the absorption coefficient K (both inter- and intraband) on the light polarization for a single nanowire or a system of parallel nanowires. The ratio of K for two light polarizations is

$$\frac{K_{\parallel}}{K_{\perp}} = \left| \frac{\varepsilon + \varepsilon_0}{2\varepsilon_0} \right|^2. \tag{2}$$

Note that so far we have considered classical electrodynamic effects caused exclusively by the difference of the refractive indices for wires and environment. In thin nanowires, due to size quantization, the optical matrix element becomes anisotropic [6,7], which may modify the described polarization effects so that Eq.(2) acquires an additional factor equal to the square of the ratio of the matrix elements for the two perpendicular directions.

$$E_z(\rho,\alpha) = E_0\sqrt{\varepsilon_0}\sum_{m=-\infty}^{\infty} i^m \frac{J_m'(ka)H_m^{(1)}(k_0a) - J_m(ka)H_m^{(1)\prime}(k_0a)}{\sqrt{\varepsilon}J_m'(ka)H_m^{(1)}(k_0a) - \sqrt{\varepsilon_0}J_m(ka)H_m^{(1)\prime}(k_0a)} J_m(k\rho)\exp(im\alpha) \tag{3}$$

Direct measurement of optical absorption in a nanowire system is difficult but it can be replaced by measurements of photoluminescence excitation or photoconductivity (for nanowires provided with contacts). All the effects discussed should be polarization-sensitive acquiring their maximum value for the exciting light polarization parallel to the nanowires. It was first observed and adequately interpreted in [8]. The authors found photoluminescence and photoconductivity in InP nanowires increasing up to 48 times when the polarization of the exciting light changed from perpendicular to parallel. This number exactly corresponds to Eq.(2) for InP in air. Similar effects with a slightly lesser degree of polarization (maybe, owing to the misorientation of the nanowires, the role of which is discussed elsewhere [9]) were also observed in luminescence of Si nanowires [10] and photoconductivity of ZnO and GaN nanowires [11,12].

Eq.(1) was initially derived for static electric fields and remains valid (together with Eq.(2)) for high frequency fields as well (with ε and ε_0 corresponding to the field frequency ω) as long as the nanowire radius a remains much less than the light wavelength both inside and outside nanowire. This condition is well satisfied in nanometer-thick nanowires of [8,10] but in those with larger diameter of about 100 nm, electrostatic formulae Eq.(1), obtained by solving the Laplace equation, become inadequate, and we should use more complicated approach to the problem of optical absorption described in more detail in [13].

We consider a cylindrical nanowire placed in an external a.c. electric field $\mathbf{E_0}$ and find the real field distribution $\mathbf{E}(\mathbf{r})$ created by $\mathbf{E_0}$ together with the nanowire-induced image forces (contrary to Eq.(1), electric field in the nanowire is no longer uniform). Then we calculate the total absorbed power proportional to $|\mathbf{E}(\mathbf{r})|^2$ integrated over the nanowire volume and study the dependence of this characteristic on the angle between $\mathbf{E_0}$ and the nanowire axis, which gives us the polarization dependence of our interest. In thick nanowires, $\mathbf{E}(\mathbf{r})$ is to be found not from the Laplace but from the Helmholtz equation $\Delta\mathbf{E} + \varepsilon\omega^2\mathbf{E}/c^2 = 0$ inside the nanowire and $\Delta\mathbf{E} + \varepsilon_0\omega^2\mathbf{E}/c^2 = 0$ outside it. The character of its solution depends on the mutual orientation of $\mathbf{E_0}$, the wavevector of light $\mathbf{k}$, and the nanowire axis $\mathbf{z}$.

For $\mathbf{k} \perp \mathbf{z}$ and $\mathbf{E_0} \parallel \mathbf{z}$, when $\mathbf{E_0} = E_0\,\mathbf{z}\exp(ik_0\rho\cos\alpha)$, the solution for $\mathbf{E}$ contains only a single component E_z. This solution can be found in [14], and we simply use its final result for the nanowire interior, $\rho < a$ (here and henceforward we omit the time-dependent factor $\exp(-i\omega t)$:where J_m and $H_m^{(1)}$ are the Bessel and first-kind Hankel functions, $k = \sqrt{\varepsilon}\,\omega/c$, $k_0 = \sqrt{\varepsilon_0}\,\omega/c$.

For $\mathbf{k}\|\mathbf{z}$ and $\mathbf{E_0}\|\mathbf{x}$, we look for a solution in the form $\mathbf{E}(\mathbf{r}) = \mathbf{E}(\rho,\alpha)\exp(ik_0z)$ and obtain for $\rho < a$:

$$\mathbf{E}(\rho,\alpha) = \frac{2E_0a\varepsilon_0\nabla\left[J_1\left(\frac{\sqrt{\varepsilon-\varepsilon_0}\,\omega\rho}{c}\right)\cos\alpha\right]}{\varepsilon_0 J_1\left(\frac{\sqrt{\varepsilon-\varepsilon_0}\,\omega a}{c}\right) + \varepsilon\frac{\sqrt{\varepsilon-\varepsilon_0}\,\omega a}{c}J_1'\left(\frac{\sqrt{\varepsilon-\varepsilon_0}\,\omega a}{c}\right)}. \tag{4}$$

At small a, Eq.(4) transforms into the static expression $\mathbf{E} = 2\varepsilon_0\mathbf{E}_0/(\varepsilon + \varepsilon_0)$ (see Eq.(1)).

As we have mentioned above, the light absorption coefficient is determined by the integral power absorbed,

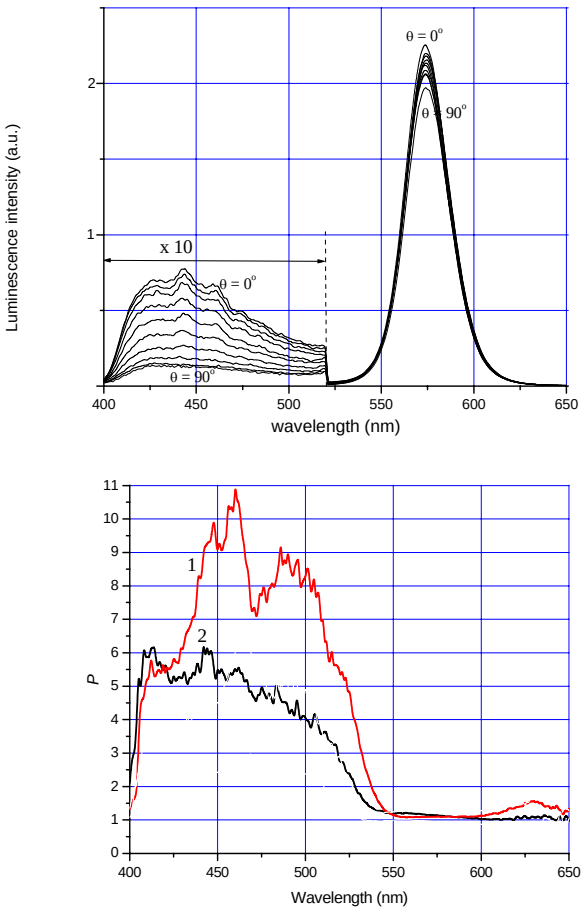

Figure 7. (a) – photoluminescence spectrum for excitation at λ = 349 nm by linearly polarized light. Different curves correspond to the luminescence components with polarization in the direction forming the angle θ with the polarization of excitation. θ increases from the upper to the lower curve with the step 10°. The amplitude of luminescence in the spectral region λ < 520 nm is shown with the magnification factor 10. (b) – spectral dependence of the ratio of luminescence intensities from Fig.3a for θ = 0° and θ = 90°, $P = I_{\parallel}/I_{\perp}$. Curves 1 and 2 correspond to the two mutually perpendicular polarizations of the exciting light, curves 3 and 4 show the same dependences in another sample.

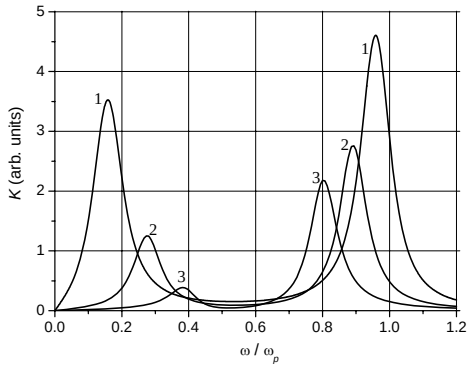

Figure 8. Absorption spectra of core-shell nanowires with p = 0.2 (1); 0.5 (2); 0.8 (3) at $\varepsilon_1 = 3$, $\nu = 0.1\omega_p$ for light polarized perpendicularly to nanowires.

proportional to $I^a = \int_0^a \int_0^{2\pi} |E(\rho,\alpha)|^2 \, d\alpha \, \rho d\rho$ (superscript a means absorption). Fig.1 shows the spectral dependences of $I_{\parallel}^a(\omega)$ (for light with parallel polarization), $I_{\perp}^a(\omega)$ (for light with perpendicular polarization) and of the ratio $P^a = \frac{I_{\parallel}^a - I_{\perp}^a}{I_{\parallel}^a + I_{\perp}^a}$ characterizing the polarization dependence of absorbed light intensity.

For $k_0 a \to 0$, this ratio tends to the electrostatic value $(\varepsilon^2 + 2\varepsilon\varepsilon_0 - 3\varepsilon_0^2)/(\varepsilon^2 + 2\varepsilon\varepsilon_0 + 5\varepsilon_0^2)$ corresponding to Eq.(2). However, at higher light frequencies (or thicker nanowires) we can no longer claim that light with parallel polarization has much higher absorption coefficient since $I_{\parallel}^a(\omega)$ and $I_{\perp}^a(\omega)$, as well as their ratio, demonstrate a strong frequency dependence. This dependence is especially dramatic for $I_{\perp}^a(\omega)$, which tends to infinity in a series of critical points corresponding to roots of the denominator Eq.(4). In our example of $\varepsilon = 9$, $\varepsilon_0 = 1$, the first of these points are $k_0 a = 0.68,\ 1.89,\ 3.02,\ldots$ Considering a cylindrical nanowire as an optical fiber [15], we can say that each of them corresponds to the cutoff of a fiber mode LP_{1m} with the same angular field distribution as Eq.(4). At the cutoff, these modes become purely transverse and excited by an incident wave. The spectrum of $I_{\parallel}^a(\omega)$ has no singularities due to the absence of modes with purely longitudinal polarization (**E** ∥ **z**).

Since an infinite value $I_{\perp}^a(\omega)$ at some fixed ω is definitely non-physical, we must discuss what initial theoretical assumptions are inadequate and what phenomena are responsible for the real height of absorption peaks. In our calculations, we have considered one single nanowire in the electric field of an infinite plane wave. In this case, the field in a nanowire can, in theory, acquire arbitrary high values remaining equal to $\mathbf{E}_0$ at very large distances. For an array of nanowires with areal density N, the field will be re-distributed between nanowires and their environment so that the total wave energy remains the same as that provided with external excitation in the absence of nanowires. Near a critical point, almost all wave energy is localized in nanowires, so that $I^a \cong \varepsilon_0 E_0^2/(\pi\varepsilon N a^2) >> 1$ is the natural upper restriction for the curve 2 at Fig.1a. There are also some other mechanisms of smoothening the mentioned singularities in $I_{\perp}^a$, e.g., non-rectilinearity and thickness fluctuations of nanowires, which may become dominant at low nanowire density.

The described frequency dependence of the polarization-sensitive absorption has not yet been studied experimentally, except for the observation [11] that two different frequencies of excited light caused different degree of photoconductivity anisotropy.

2.2. Metallic nanowires

Similar polarization phenomena in the light absorption can be observed not only in semiconductor but also in

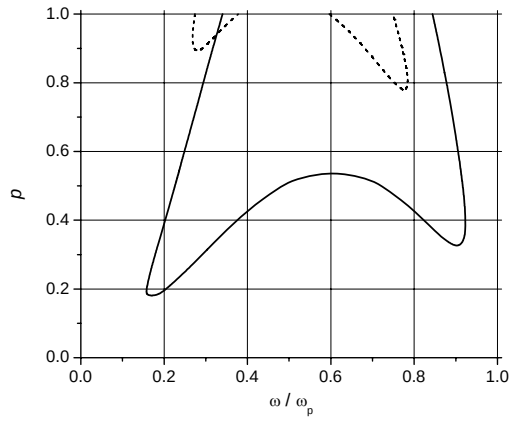

Figure 9. Values of p and ω, for which $E_\perp = E_{0\perp}$ at $\varepsilon_1 = 3$ (solid line) and $\varepsilon_1 = 10$ (dashed lines). The area above the line(s) corresponds to $E_\perp > E_{0\perp}$.

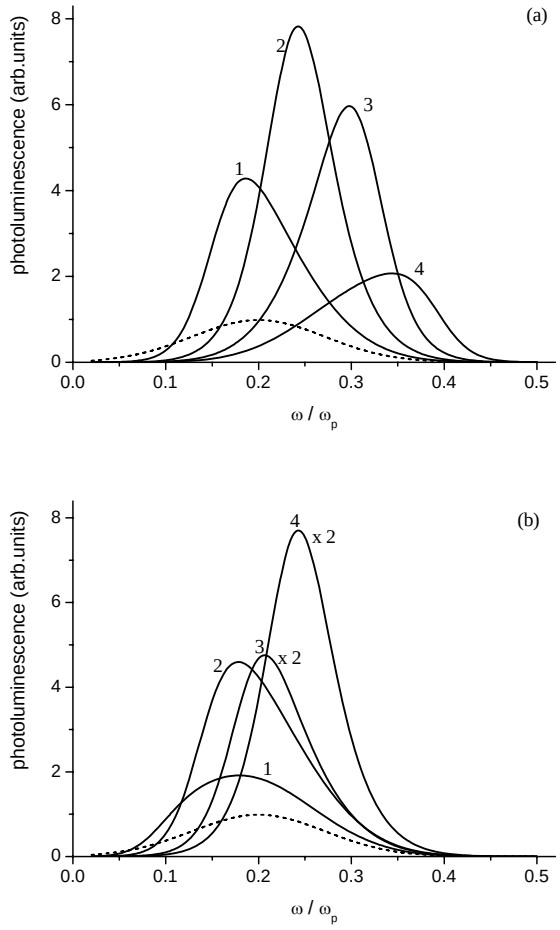

Figure 10. Amplification and spectral shift of a luminescence line with $\omega_{em} = 0.2\ \omega_p$ for an effective dipole perpendicular to the axis of a core-shell nanowire with $\varepsilon_1 = 3$ (a) and $\varepsilon_1 = 10$ (b). Dashed lines correspond to the absence of a metallic shell ($p = 0$), solid lines to a different relative volume of a shell: 1 – p = 0.2; 2 – p = 0.4; 3 – p = 0.6; 4 – p = 0.8.

metallic nanowires. The main difference consists in the fact that, due to a strong frequency dispersion of ε in metals related to the plasmon phenomena, polarization characteristics depend on the light frequency even in arbitrary thin nanowires. To analyze these phenomena theoretically, we use for ε the simplest Drude expression $\varepsilon = 1 - \frac{\omega_p^2}{\omega(\omega - i\nu)}$ where ω_p is the plasma frequency and ν is the scattering rate.

It can be seen from Eq.(1) that at $\omega \to \omega_p / \sqrt{\varepsilon_0 + 1}$ the field component $E_\perp$ inside nanowires increases dramatically, being restricted only by the non-zero scattering rate of carriers, which, in turn, results in a noticeable absorption in this spectral region. This is the manifestation of well known plasmon effects in nanostructures [16] which in our extremely anisotropic case, occur only for light polarized perpendicular to the nanowire axis. As a result, anisotropy of optical absorption given by Eq.(2), in metallic nanowires has an interesting spectral dependence. Far below the plasmon frequency (which in most metals corresponds to infrared radiation and the red part of visible spectrum), |ε(ω)| is very large, and the situation is similar to that in thin semiconductor nanowires where absorption is much higher for the light with parallel polarization. However, near the plasmon frequency absorption of the perpendicularly polarized light increases dramatically, changing the sign of anisotropy, as illustrated by the solid curve at Fig.2.

Thus, the situation near the plasmon resonance is, to some extent, opposite to that in thin semiconductor nanowires where, due to large ε, electric field of light is polarized mostly along the wire axis. In metallic nanowires, ε for light polarized perpendicular to the wires and having a frequency in the plasmon region is close to zero. For this reason, the electric field in a wire will have essentially normal polarization which makes plasmon phenomena noticeable for arbitrary light polarization.

Though the described spectral dependences of absorption are very specific and interesting, their experimental observation is more difficult than for the effects in semiconductor nanowires. In metals we can measure neither photoconductivity nor luminescence excitation and have to restrict ourselves to direct measurements of optical absorption. The most straightforward method to do it is to investigate large number of nanowires suspended in some liquid optically inactive in the spectral region of interest. In this case, orientation of nanowires is random, and no polarization dependence should be observed. Strong anisotropy of absorbing objects will be revealed only in a specific character of spectral dependence of the absorption coefficeint (Fig.3). In this spectrum strong low-frequency absorption is caused by nanowires almost parallel to the light polarization while the plasmon maximum is formed by those with orientation close to the perpendicular one.

2.3. Nanorods

The term "nanorods" is typically applied to solution-grown nanocrystals having essentially non-spherical, elongated shape and fabricated quite easily from both semiconducting [17] and metallic [18] materials. They are characterized by qualitatively the same polarization phenomena as mentioned above for nanowires but have two quantitative distinctions. First, nanorods are characterized by smaller dimensions, typically not exceeding several nanometers, which makes quantum size phenomena, mentioned after Eq.(2), more noticeable and existing not only for the transversal, but also for the longitudinal motion of carriers. Second, nanorods have the aspect ratio a/b usually not exceeding 2-5, which is much less than that of nanowires reaching several hundreds. The last factor makes the theoretical description used in the present work and based on the model of infinitely long cylinder, quantitatively inadequate.

For a more correct treatment, nanorods can be considered as prolate ellipsoids of rotation with the semi-axes a, b, and b ($a > b$). Electrodynamics of this body is characterized by the so-called depolarization factors $n_{\|}$ and $n_{\perp}$ where [5]:

$$n_{\|} = \frac{(b/a)^2}{[1-(b/a)^2]^{3/2}}\left[\operatorname{Arctanh}\sqrt{1-(b/a)^2} - \sqrt{1-(b/a)^2}\right]; \quad n_{\perp} = \frac{1-n_{\|}}{2}. \tag{5}$$

In terms of these factors, Eq.(1) should be re-written in the form

$$E_{\|} = \frac{E_{0\|}}{1+(\varepsilon/\varepsilon_0-1)n_{\|}}; \qquad E_{\perp} = \frac{E_{0\perp}}{1+(\varepsilon/\varepsilon_0-1)n_{\perp}}. \tag{6}$$

For infinitely long nanowires ($a >> b$), $n_{\|} = 0$, $n_{\perp} = ½$, and we return to Eq.(1). By using Eq.(6), it is easy to generalize Eq.(2) and other formulae for thin nanowires, to the case of nanorods.

3. Polarization of luminescence

In the previous section we considered physical phenomena related to the fact that external non-polarized light becomes strongly polarized inside a nanowire with high refractive index. Now we discuss the related problem of polarization of light emitted by a nanowire. As a first step, we solve the auxiliary problem of finding the electric field created by an electric dipole placed at the axis of a cylinder with radius a and dielectric constant ε, in environment with ε_0. The result depends on the orientation of the dipole moment $\mathbf{d}_0$ relative to the cylinder axis (z-axis), and we consider separately the cases $\mathbf{d}_0 \| \mathbf{z}$ and $\mathbf{d}_0 \perp \mathbf{z}$. In the static limit $k_0 a << 1$, the answer is quite simple [9]: for $\mathbf{d}_0 \| \mathbf{z}$, the electric field of the radiation far from the nanowire, has the same amplitude and configuration as would be created by a dipole with the moment $\mathbf{d}_0$ in free space. For the normal orientation of $\mathbf{d}_0$, the corresponding effective moment is given by $\mathbf{d} = 2\varepsilon_0\mathbf{d}_0/(\varepsilon+\varepsilon_0)$. As a result, even for nanowires with isotropic interband matrix elements (which is definitely the case for cubic semiconductors and for moderate a when size quantization only plays a minor role), where otherwise luminescence should be non-polarized, it acquires a strong polarization under the influence of image forces.

For thick nanowires, we can use the general approach described in [19] for a similar problem, which allows us to present only the final expression for resulting electric field outside the nanowire. In the case of parallel dipole orientation ($d_0 = d_{0z}$), the electric field E_z is independent of α and at $\rho > a$ is given by

$$E_z = i\frac{d_{0z}}{\varepsilon}\int_{-\infty}^{\infty} \frac{J_1(k_\rho a)H_0^{(1)}(k_\rho a) - J_0(k_\rho a)H_1^{(1)}(k_\rho a)}{J_1(k_\rho a)H_0^{(1)}(k_{\rho 0}a) - \frac{k_{\rho 0}}{k_\rho}J_0(k_\rho a)H_1^{(1)}(k_{\rho 0}a)} k_\rho^2 \exp(ik_z z)H_0^{(1)}(k_{\rho 0})dk_z. \tag{7}$$

Here $k_\rho = \sqrt{\varepsilon\omega^2/c^2 - k_z^2}$, $k_{\rho 0} = \sqrt{\varepsilon_0\omega^2/c^2 - k_z^2}$.

To analyze the intensity of emitted light far from the nanowire (at $\rho >> k_0^{-1}$), we use the asymptotic formula for $H_0^{(1)}$ and calculate the integral in Eq.(7) using the stationary phase method. This Gives

$$E_z \approx \frac{d_{0z}\omega^2}{\varepsilon c^2 r}(\varepsilon - \varepsilon_0\cos^2\theta)\exp(ik_0 r + i\pi/4)\frac{J_1(k_\rho^0 a)H_0^{(1)}(k_\rho^0 a) - J_0(k_\rho^0 a)H_1^{(1)}(k_\rho^0 a)}{J_1(k_\rho^0 a)H_0^{(1)}(k_{\rho 0}^0 a) - \frac{k_{\rho 0}^0}{k_\rho^0}J_0(k_\rho^0 a)H_1^{(1)}(k_{\rho 0}^0 a)} \tag{8}$$

where $k_\rho^0 = k_0(\varepsilon/\varepsilon_0 - \cos^2\theta)^{1/2}$, $k_{\rho 0}^0 = k_0\sin\theta$, $r = (\rho^2 + z^2)^{1/2}$ is the distance from the dipole, and $\theta = \arccos(z/r)$ is the angle from the nanowire axis.

If we consider light emission perpendicular to the dipole where $\theta = \pi/2$, the corresponding electric field will have the same coordinate dependence as that of a free dipole ~ $(d_{0z}\omega^2/c^2 r)\exp(ik_0 r)$ with some additional factor given by

the fraction in Eq.(8). Thus, the influence of image forces is equivalent to the replacement of d_{0z} with some effective dipole

$$d_z = d_{0z}\sqrt{\varepsilon}\,\frac{J_1(ka)H_0^{(1)}(ka) - J_0(ka)H_1^{(1)}(ka)}{\sqrt{\varepsilon}J_1(ka)H_0^{(1)}(k_0a) - \sqrt{\varepsilon_0}J_0(ka)H_1^{(1)}(k_0a)} \equiv A_z d_{0z}. \quad (9)$$

For the perpendicular dipole orientation ($d_0 = d_{0x}$), similar calculations give

$$d_x = d_{0x}\sqrt{\varepsilon}\,\frac{J_1'(ka)H_1^{(1)}(ka) - J_1(ka)H_1^{(1)}{}'(ka)}{\sqrt{\varepsilon_0}J_1'(ka)H_1^{(1)}(k_0a) - \sqrt{\varepsilon}J_1(ka)H_1^{(1)}{}'(k_0a)} \equiv A_x d_{0x}. \quad (10)$$

Fig.4 shows the frequency dependence of the effective dipoles d_x, d_z and of their ratio. At $\omega \to 0$ they acquire the static values $d_z = d_{0z}$, $d_x = 2\varepsilon_0 d_{0x}/(\varepsilon+\varepsilon_0)$, and then demonstrate strong oscillations. At larger ω (or larger a), the phases of oscillations close in, d_z approaches d_x, so that the radiation becomes almost unpolarized.

So far we have analyzed the emission characteristics of one single effective dipole in a nanowire. To obtain radiation characteristics of the whole nanowire, we must perform integration over its length assuming the dipoles distributed uniformly along *z*. As a result, light emitted, say, in **y** direction and polarized along **x** is, indeed, generated only by d_x dipoles. At the same time, light with **z** polarization contains contributions from both d_z and d_y dipoles (in cylindrical nanowires $d_y = d_x$). As shown in [9], the intensity ratio for different light polarization

$$\frac{I_{\parallel}^e}{I_{\perp}^e} = \frac{d_x^2 + 2d_z^2}{3d_x^2} \quad (11)$$

(superscript *e* means emission). Spectral dependence of the resulting polarization ratio $P^e = \dfrac{I_{\parallel}^e - I_{\perp}^e}{I_{\parallel}^e + I_{\perp}^e}$ calculated with Eqs.(9)-(11) for isotropic internal emission ($d_{0x} = d_{0z}$) is shown in Fig.5. This is seen to have a strong oscillatory character changing sign at some critical frequencies differing from those in the polarization dependence of absorption (Fig.1).

Strong polarization of luminescence from nanowires with $\varepsilon \neq \varepsilon_0$ was clearly demonstrated experimentally [8,10]. The effect is qualitatively similar to the property of absorption considered in Sec.2 but the magnitude of polarization is different. By comparing Eq.(11) with Eq.(2) one can see that in the static limit, where $\dfrac{d_x^2 + 2d_z^2}{3d_x^2} = \dfrac{(\varepsilon+\varepsilon_0)^2 + 2\varepsilon_0^2}{6\varepsilon_0^2}$, the degree of polarization for luminescence is less than for absorption. It is caused by the fact that, according to Eq.(11), light with parallel polarization is generated not only by d_z dipole moments but also by d_x which are weakened by image forces. E.g., for thin InP nanowires (ε =12.7) we get $K_{\parallel}/K_{\perp}$ = 49, $I_{\parallel}^e/I_{\perp}$ = 30, in good agreement with the experimentally observed values of $K_{\parallel}/K_{\perp}$ = 48, $I_{\parallel}^e/I_{\perp}$ = 24 [8].

In thick nanowires, according to Fig.5, the polarization of luminescence should oscillate with ω. If, for instance, the luminescence spectrum of a nanowire material contains several lines with noticeably different frequencies (as, say, in ZnSe [20] or ZnO [11] nanowires where interband and impurity transitions may cause emission with frequencies differing by 1.3-1.7 times and comparable intensities), the polarization of these lines can be essentially different and even have opposite sign, as it was observed in ZnO nanowires [21].

4. Polarization memory

4.1. Theoretical considerations

So far we have considered optical characteristics of a single nanowire. In many cases real nanowire structures are comprised of arrays of many parallel nanowires and the absorption or luminescence is a sum of their individual contributions. If the nanowires are parallel, all the previous expressions can adequately describe the behavior of such an whole array since the terms "parallel" or "perpendicular" polarization have the same meaning for all nanowires. We implicitly used this fact when comparing the single-wire formulae with experimental data for systems of parallel nanowires. In the case of an array of randomly oriented nanowires (say, nanowires in a polymer matrix of in solution), the system has macroscopically isotropic optical properties but simultaneously must possess a very interesting property of polarization memory. If we excite photoluminescence in the system using polarized light, in accordance with Sec.2.1, non-equlibrium carriers in thin semiconductor nanowires will be generated mostly in those that are oriented close to parallel to the light polarization. According to Sec.3, light emitted by these nanowires will have preferable polarization parallel to them, or in other words, parallel to the polarization of the exciting radiation. This effect was discussed theoretically in [9,22] and observed experimentally in porous Si structures [23] where the condition $k_0a << 1$ is satisfied.

In metallic or thick semiconductor nanowires the polarization characteristics for absorption and emission were shown to vary dramatically with the light frequency. This allows us to expect that the polarization memory must demonstrate strong dependence on the frequency of both

exciting (ω_{ex}) and emitted (ω_{em}) light and even change its sign at some intervals of ω_{ex} and ω_{em}.

We present here a brief outline of its theoretical description [13] based on our earlier analysis [9] of the limiting case $k_0a << 1$. We assume that a random array of nanowires is excited by *z*-polarized light with frequency ω_{ex} while our detector is placed at some point $(0,y_0,0)$ outside the array. By symmetry, the Poynting vector of resulting luminescence **S** is directed along the *y*-axis and is given by the sum of S_y components created by all nanowires. Consider a single nanowire with orientation characterized by spherical angles θ and α. According to [9], the ratio of S_y for the light with *z*-and *x*-polarization (parallel and perpendicular to the exciting light polarization) is

$$\frac{\left(S_y\right)_z}{\left(S_y\right)_x}=\frac{\left(d_x^2+2d_z^2\right)\cos^2\theta\left(\cos^2\theta+\sin^2\theta\sin^2\alpha\right)+3d_x^2\sin^2\theta\sin^2\alpha}{\left(d_x^2+2d_z^2\right)\sin^2\theta\sin^2\alpha\left(\cos^2\theta+\sin^2\theta\sin^2\alpha\right)+3d_x^2\cos^2\theta} \qquad (12)$$

where in our case d_x and d_z are given, respectively, by Eq.(10) and Eq.(9) with the frequency ω equal to ω_{em}.

If all nanowires emitted with the same intensity, then averaging the numerator and denominator of Eq.(12) over all angles would give unity (non-polarized radiation). However, according to Sec.2a, the intensity of absorbed exciting light and hence the intensity of luminescence depends on θ being proportional to $\left(I_{\parallel}^{a}\cos^2\theta+I_{\perp}^{a}\sin^2\theta\right)$ where $I_{\parallel}^{a}$ are determined by the expressions of Sec.2.1 with $\omega = \omega_{ex}$. Performing angular integration in Eq.(12) with this weighting factor, we eventually obtain the ratio of luminescence intensities with polarization parallel and perpendicular to that of the exciting light:

$$\frac{I_{\parallel}^{e}}{I_{\perp}^{e}}=\frac{2I_{\perp}^{a}(\omega_{ex})\left[47d_x^2(\omega_{em})+10d_z^2(\omega_{em})\right]+3I_{\parallel}^{a}(\omega_{ex})\left[13d_x^2(\omega_{em})+12d_z^2(\omega_{em})\right]}{4I_{\perp}^{a}(\omega_{ex})\left[16d_x^2(\omega_{em})+11d_z^2(\omega_{em})\right]+3I_{\parallel}^{a}(\omega_{ex})\left[23d_x^2(\omega_{em})+4d_z^2(\omega_{em})\right]}. \qquad (13)$$

To avoid misunderstanding, we emphasize the difference in notations between Eq.(13) and Eq.(11) where $I_{\parallel}^{e}$ and $I_{\perp}^{e}$ referred to the light polarized parallel and perpendicular to the nanowire axis.

Fig.6 shows the dependences of the system polarization ratio $P^e=\dfrac{I_{\parallel}^{e}-I_{\perp}^{e}}{I_{\parallel}^{e}+I_{\perp}^{e}}$ on the frequencies of exciting (ω_{ex}) and emitted (ω_{em}) light [13]. Formally, calculations can be performed for an arbitrary relationship between ω_{ex} and ω_{em}. Since, however, in standard photoluminescence measurements ω_{ex} always exceeds ω_{em}, parts of the curves in Fig.6 where this condition is violated, are given by dashed lines. At ω_{ex}, $\omega_{em} \to 0$ polarization tends to its low-frequency limit calculated in [9] which for our choice $\varepsilon/\varepsilon_0 = 9$ is equal to $P^e \approx 0.40$ and in the limit $\varepsilon/\varepsilon_0 \to \infty$ tends to 0.5.

It is important to mention that if the nanowire material is characterized by several luminescence lines with essentially different frequencies, then these lines may have different degree of polarization, in accordance with Fig.5a. Since the curve at the figure crosses the level $P^e = 0$ (or $I_{\parallel}^{e} = I_{\perp}^{e}$), there exists even the possibility when one of these lines is polarized along and another – perpendicular to the polarization of exciting light.

4.2. Polarization memory in semiconductor nanorods (experiment)

Experimental investigation of polarization memory in nanorods [24] was performed at core-shell CdSe/ZnS heterostructures – the system with elaborated technology of growing high-quality nanocrystals. Statistical analysis of microscopic images gives the following values for nanorod dimensions and their dispersion: diameter $2b$ = 3.67±0.47 nm, length $2a$ = 8.57±0.85 nm, which results in the aspect ratio a/b = 2.37±0.33. For optical measurements nanorods were dissolved in chloroform.

To investigate the polarization memory, the samples were optically excited by a polarized light with λ = 366 nm. The luminescence spectrum presented at Fig.7a consists of two peaks. The ground state peak λ = 573 nm corresponds to the effective bandgap E_g = 2.16 eV, which for our CdSe nanorods is in a complete agreement with the comprehensive data table of [25]. The short wavelength peak, centered around 450 nm, in the luminescence spectra has essentially lower amplitude and some additional structure. Polarization properties of the emitted light presented at Fig.7a in the form of luminescence spectra for different angular positions of the analyzer related to the direction of exciting light polarization **e**. The luminescence is seen to be polarized mostly parallel to **e** and the degree of this polarization is much higher in the short wavelength peak that in the long wavelength one. It is especially clear from Fig.7b where the curve 1 shows the spectral dependence of the polarization degree $P = I^e_{\parallel}/I^e_{\perp}$ representing the intensity ratio of luminescence with polarization parallel and perpendicular to **e** for the data given in Fig.7a.

To attribute unequivocally the observed regularities to the polarization memory, we need an additional confirmation that the polarization of luminescence is not related to an internal anisotropy of a system, which might be due to the mutual alignment of NR forming a system similar to liquid crystals. For this purpose, we repeated the whole series of luminescent measurements for the excitation polarization

rotated by 90° from the initial position. The corresponding spectrum of polarization degree is also given at Fig.3b. The two curves differ quantitatively, presumably due to some mismatch in polarization measurements and/or system anisotropy. However, their qualitative behavior is strictly similar confirming: (*i*) existence of the polarization memory and (*ii*) its different amplitude for different luminescence peaks.

The last experimental fact requires a special discussion and explanation. If the two luminescence peaks correspond to different types of optical transitions in a nanorod, the observed difference in polarization memory should be attributed to different anisotropy of corresponding optical matrix elements. In the absence of this anisotropy, the dielectric constant mismatch must result in preferable absorption and emission of light polarized parallel to the nanorod axis with the same optical memory for all transitions. Our experimental results could be explained if the matrix element responsible for the ground state 573 nm line is larger for perpendicular light polarization (it is really the case for NR with a small aspect ratio [26]) while that for the 470 nm line is either more isotropic or larger for parallel polarization. This is in qualitative agreement with the theoretical [27] and experimental [28] conclusions of essentially different polarization properties of different optical transitions in NR. More detailed comparison of the theory and experiments is difficult since our samples were characterized by the aspect ratio belonging to the critical region a/b = 2-3 where the energy spectrum and polarization characteristics of CdSe NR suffer dramatic changes [26].

There is one more mechanism, which can be partially responsible for different polarization degree of different luminescence peaks. Theoretical calculations of the polarization memory [9,22,23] used the formulae for electric field redistribution caused by one single nanorod and hence are adequate only for strongly diluted solutions. In real systems, fields of neighboring nanorods interact, and measurable optical characteristics are determined by some effective averaging over a domain with characteristic size of order of the light wavelength. Such averaging may result in some isotropization of effective absorbers/emitters suppressing the polarization memory. For a given nanorod system, the number of nanorods in such domain becomes larger and the polarization smaller with the increase in wavelength. We may assume that this effect is also responsible for the decrease of P with the emitted light wavelength observed in porous Si [23].

5. Core-shell nanowires

5.1. Field distribution

Now we generalize some of the obtained results to the case of core-shell nanowires containing two coaxial regions with different dielectric constants. We consider a nanowire consisting of the central core having radius ρ_1 and dielectric constant ε_1 and the shell with radius $\rho_2 > \rho_1$ and dielectric constant ε_2. For simplicity, we restrict ourselves to the thin-wire static case $k_0 a << 1$. In this case, an external electric field $\mathbf{E}_0$ perpendicular to the wire axis creates in the core a uniform field

$$\mathbf{E}_1 = \frac{4\varepsilon_0\varepsilon_2\mathbf{E}_0}{2\varepsilon_2(\varepsilon_1+\varepsilon_2)+p(\varepsilon_2-\varepsilon_1)(\varepsilon_2-\varepsilon_0)} \equiv A\mathbf{E}_0 \quad (14)$$

where $p = 1 - (\rho_1/\rho_2)^2$ is the ratio of shell volume to total nanowire volume. The field in the shell is a sum of a uniform field and that of a linear dipole:

$$\mathbf{E}_2 = \frac{2\varepsilon_0}{2\varepsilon_2(\varepsilon_1+\varepsilon_2)+p(\varepsilon_2-\varepsilon_1)(\varepsilon_2-\varepsilon_0)}\left\{(\varepsilon_1+\varepsilon_2)\mathbf{E}_0 + 2(\varepsilon_2-\varepsilon_1)(\varepsilon_2-\varepsilon_0)r_1^2\left[\frac{\mathbf{E}_0}{\rho^2}-\frac{2\mathbf{r}(\mathbf{r}\mathbf{E}_0)}{\rho^4}\right]\right\} \quad (15)$$

For $\mathbf{E}_0$ parallel to the wire axis, $\mathbf{E}_1 = \mathbf{E}_2 = \mathbf{E}_0$.

Formulae Eqs.(14),(15) can be used to determine the spectra and polarization dependence of optical phenomena in core-shell nanowires. We will not analyze the cases when the core and the shell are both semiconducting or both metallic since they have no qualitative difference with the effects considered above. The situation is different for nanowires with a metallic shell and a semiconductor core. We will see that the plasmon spectra of such systems differ noticeably from those in uniform metallic nanowires and, besides, mutual influence of plasmon effects in a shell and luminescent phenomena in a core results in new effects and new functional possibilities of such structures.

Specific features of the optical response of metallic nanoshells arises from the fact that the plasmon absorption maximum existing in the entire metallic shell is split into two maxima with positions depending on the relationship between r_1 and r_2 for the light with perpendicular polarization [9]. The frequency regions near the plasmon resonances are characterized by anomalously high electric field strength (light amplification) both in the core and in the shell. As it has been already pointed out for core-shell nanodots [29], this can be used for enhancement of non-linear optical effects in a core (in our case – only for light with a perpendicular polarization). There is also a reciprocal effect: an oscillating dipole $\mathbf{d}_0$ in the core creates outside the wire radiation field which may be much larger than that in a uniform medium.

5.2. Optical absorption

To calculate the optical absorption in a core-shell nanowire caused by light with perpendicular polarization, we must include the local absorption $\mathrm{Im}\varepsilon_2 |\mathbf{E}_2(\rho)|^2$ and integrate it over the whole shell. Using the Drude formula for ε_2, we obtain the absorption spectra for this polarization, $K_\perp(\omega)$. Comparing them with the monotonic $K_\parallel(\omega)$, coinciding

with that in bulk metals, we get the polarization curves also presented in Fig.2. In accordance with the previous paragraph, they demonstrate the presence of two minima corresponding to two plasmon modes. With increasing p, the minima approach each other so that at $p \to 1$ we get a single plasmon resonance near $\omega = \omega_p/\sqrt{2}$ typical for a long metallic cylinder.

If the core is a semiconductor with the bandgap $E_g < \hbar\omega$, then, besides the absorption described above, there is also interband absorption in the core proportional to $|\mathbf{E}_1|^2$. The magnitudes of absorption in a shell and a core depend on different parameters (i.e., the plasma frequency and scattering rate in metals, and band gap width and interband matrix element in semiconductors) and thus the absorption spectrum and its polarization properties have no universal character, which makes the optical absorption data quite ambiguous for analysis. The problem can be solved by measuring the excitation spectra for core luminescence. In composite nanostructures, those are proportional only to the partial absorption in the core and thus differ from the absorption spectra. We discuss briefly polarization characteristics of the mentioned excitation spectra.

As we have shown in Sec.2, thin semiconductor and metallic nanowires have an opposite character of electrical anisotropy (and hence of polarization properties): the perpendicular component of the electric field is suppressed as compared with the parallel one, in a semiconductor nanowire, and enhanced in a metallic nanowire in the vicinity of a plasmon frequency. In composite core-shell structures, both variants can be realized, depending on the shell thickness and light frequency. The corresponding "phase diagram" using p-ω axes, is shown in Fig.9. The areas above the line(s) correspond to the "metallic" case $E_\perp > E_{0\perp}$ while those below the line(s) – to the "semiconductor" case $E_\perp < E_{0\perp}$. In other words, these lines correspond to $|A| = 1$where the factor is given by Eq.(14). At small p, one naturally deals with the "semiconductor" regime. One might be surprised that at $p \to 1$ the regime is not "metallic" but it should be pointed that the figure describes the field not in a metallic shell, but in a semiconductor core, which in the limit of a pure metallic nanowire simply disappears.

The condition $|A| > 1$ is satisfied in the vicinity of plasmon resonances, which means that for light inducing interband absorption in the core, the intensity of electron-hole pair generation and, hence, the intensity of luminescence caused by these pairs is larger than in the absence of a metallic shell. That is why we call A the "amplification factor".

5.3. Luminescence amplification

We have just mentioned the possible role of metallic shells in amplification of the a.c. electric field of the exciting light due to the influence of image forces. Now we discuss the influence of shells on the direct emission of light by a semiconductor core. The a.c. electric field emitted by a core, which can be considered as an effective dipole $\mathbf{d}_0$, is disturbed by a metallic shell so that the field far from the nanostructure looks like one created by some other effective dipole **d**. By analogy with the previous section, we may expect that in the vicinity of a plasmon resonance the condition $|d/d_0| > 1$ can be realized, which means an effective amplification of the emitted radiation as well. The calculations show [9] that luminescence of core-shell structures is characterized by exactly the same rules as absorption. The field of dipoles parallel to the nanowire axis is not disturbed by image forces, while the field of perpendicular dipoles acquires the additional factor A. As a result, for an isotropic distribution of effective dipoles, such as in a cubic semiconductor core in the absence of size quantization, the emission from a nanowire acquires a partial polarization parallel to the wire axis at $|A| < 1$ or perpendicular at $|A| > 1$. Since A has a strong frequency dependence, the components of emitted light with different polarization may have different spectra depending on the metallic shell parameters.

For an effective dipole d_{0x} perpendicular to the axis of a core-shell nanowire, the real luminescence spectrum is determined by the product of the bare luminescence spectrum $|d_{0x}(\omega)|^2$ and the spectrum of $|A(\omega)|^2$. To demonstrate the role of a metallic shell, we performed calculations assuming $|d_{0x}(\omega)|^2$ to have a Gaussian shape with the centre at $\omega_{em}=0.2\omega_p$ and the width $0.1\omega_p$. Calculations show that for reasonable parameters of nanoshells, the lower plasmon peak may lie both left and right of this ω_{em}. Fig.10 shows the resulting transformation of the luminescence spectrum for perpendicular to a nanowire polarization. The most remarkable but anticipated result consists of a dramatic increase in the luminescence intensity near the resonance condition when the plasmon frequency coincides with ω_{em}. Another interesting feature is the shifting of the frequency of the luminescence line in off-resonant conditions. From the practical point of view, the results of Fig.9 demonstrate that by using metallic shells we can increase multifold the intensity of nanowire luminescence and shift the spectral position of a luminescent line. Qualitatively similar effects for core-shell nanodots have been recently predicted in [30].

For cubic semiconductors and the absence of size quantization in the core, $d_{0x} = d_{0z}$, and the dashed curve at Fig.8 gives directly $|d_{0z}(\omega)|^2$. As a result, comparing it with the corresponding solid curve and using Eq.(11), we get directly polarization of the emitting radiation and its frequency dependence.

It would be very attractive to enhance the photoluminescence dramatically by a simultaneous amplification of both exciting and emitting light. Such a situation often occurs in surface-enhanced Raman scattering but in luminescence its realization is more difficult since the difference in frequencies of exciting ω_{ex} and emitted ω_{em} light is usually quite large. They can be covered by a single plasmon peak only if the latter is wide enough, which can be realized only at large enough ν which corresponds to a low level of amplification. An alternative possibility consists in using both plasmon peaks. In this case the shell parameters should be chosen in

such a way that the low-frequency peak corresponds to ω_{em} in a given nanowire core while the source of excitation is tuned for ω_{ex} to coincide with the second peak lying near ω_p, which for most metals belongs to the ultraviolet spectral region.

References

[1] X. Duan, C.M. Lieber, *Adv. Mater.* **12**, 298 (2000)
[2] X. Mei, M. Blumin, M. Sun, D. Kim, Z.H. Wu, H.E. Ruda, Q.X. Guo, *Appl. Phys. Lett.* **82**, 967 (2003).
[3] L.J. Lauhon, M.S. Gudiksen, D. Wang, C.M. Lieber, *Nature* **420**, 57 (2002).
[4] H.-J. Choi, J.C. Johnson, R. He, S.-K. Lee, F. Kim, P.Pauzauskie, J. Goldberger, R.J. Saykally, P. Yang, *J. Phys. Chem. B* **107**, 8721 (2003).
[5] L.D. Landau, E.M. Lifshits, *Electrodynamics of Continuous Media* (Pergamon, New York, 1984).
[6] P.C. Sercel, K.J. Vahala, *Appl. Phys. Lett.* **57**, 545 (1990).
[7] C.R. McIntyre, L.J. Sham, *Phys. Rev. B* **45**, 9443 (1992).
[8] J. Wang, M.S. Gudiksen, X. Duan, Y. Cui, C.M. Lieber, *Science* **293**, 1455 (2001).
[9] H.E. Ruda, A. Shik, *Phys. Rev. B* **72**, 115308 (2005).
[10] J. Qi, A.M. Belcher, J.M. White, *Appl. Phys. Lett.* **82**, 2616 (2003).
[11] Z. Fan, P.-C. Chang, J.G. Lu, E.C. Walter, R.M. Penner, C.-H. Lin, H.P. Lee, *Appl. Phys. Lett.* **85**, 6128 (2004).
[12] S. Han, W. Jin, D. Zhang, T. Tang, C. Li, X. Liu, Z. Liu, B. Lei, C. Zhou, *Chem. Phys. Lett.* **389**, 176 (2004).
[13] H.E. Ruda, A. Shik, *J. Appl. Phys.* **100**, 024314 (2006).
[14] V.V. Batygin, I.N. Toptygin, *Problems in Electrodynamics* (Academic Press, 1978).
[15] J.A. Buck, *Fundamentals of Optical Fibers* (J. Wiley & Sons, New York, 2004).
[16] U. Kreibig, M. Vollmer, *Optical Properties of Metal Clusters* (Springer, Berlin, 1995).
[17] A.P. Alivisatos, *Science* **271**, 933 (1996).
[18] Y.Y. Yu, S.S. Chang, C.L. Lee, C.R.C. Wang, *J. Phys. Chem. B* **101**, 661 (1997).
[19] Weng Cho Chew, *Waves and Fields in Inhomogeneous Media* (Van Nostrand Reinhold, Amsterdam, 1990).
[20] U. Philipose, H.E. Ruda, A. Shik, C.F. de Souza, P. Sun, *Proc. SPIE* **5971**, 597116 (2005).
[21] N.E. Hsu, W.K. Hung, Y.F. Chen, *J. Appl. Phys.* **96**, 4671 (2004).
[22] P. Lavallard, R.A. Suris, *Solid State Comm.* **95**, 267 (1995).
[23] D. Kovalev, M. Ben Chorin, J. Diener, F. Koch, Al.L. Efros, M. Rosen, N.A. Gippius, S.G. Tikhodeev, *Appl. Phys. Lett.* **67**, 1585 (1995).
[24] E. Kravtsova, U. Krull, S. Musikhin, H.E. Ruda, A. Shik, *Appl. Phys. Lett.* (in press).
[25] L. Li, J. Hu, W. Yang, A.P. Alivisatos, *Nano Lett.* **1**, 349 (2001).
[26] J. Hu, L.-S. Li, W. Yang, L. Manna, L.-W. Wang, A. P. Alivisatos, *Science* **292**, 2060 (2001).
[27] J. Li, L. Wang, *Nano Lett.* **3**, 101 (2003).
[28] N. Le Thomas, E. Herz, O. Schöps, U. Woggon, M.V. Artemyev, *Phys. Rev. Lett.* **94**, 016803 (2005).
[29] A.E. Neeves, M.H. Birnboim, *J. Opt. Soc. Am. B* **6**, 787 (1989).
[30] H.E. Ruda, A. Shik, *Phys. Rev. B* **71**, 245328 (2005).